

Pressure-induced insulator to metal transition in amorphous SiO

A. Pesach,¹ R. Shuker,¹ and E. Sterer²

¹*Physics Department, Ben Gurion University of the Negev, P. O. Box 563, Beer Sheva 84105, Israel*

²*Nuclear Research Center-Negev, P. O. Box 84109, Beer-Sheva, Israel*

(Received 13 June 2007; revised manuscript received 20 September 2007; published 12 October 2007)

We have observed an insulator to metal transition in amorphous silicon monoxide at a critical pressure of $P_c \sim 12$ GPa as deduced from the temperature dependence of the electrical resistance and ir and Raman spectroscopies. X-ray scattering data indicate a disordered material at pressures below and above the transition to the metallic state and up to 30 GPa. Above P_c , dR/dT becomes positive, and the ir and Raman spectra flatten, indicating delocalization of nonbonding states. The temperature dependence of the conductivity is in very good agreement with the Anderson model for amorphous materials.

DOI: [10.1103/PhysRevB.76.161102](https://doi.org/10.1103/PhysRevB.76.161102)

PACS number(s): 71.30.+h, 72.15.Cz

I. INTRODUCTION

The vast research on SiO during recent years (compiled in the appendix of Ref. 1) does not give an explicit description concerning its structural properties. We find it most intriguing to observe its various physical characteristics, and in particular its electronic state and electrical conduction under high pressure. It is more so as this compound exhibits x-ray scattering patterns compatible with disordered materials in the pressure range up to 30 GPa. The IV-VI group (IV=Si, Ge, Sn, Pb; VI=O, S, Se, Te) has been studied extensively in the past,² including under high pressure, with the exception of SiO and GeO, which are metastable solids. The divalence of the chalcogenides in these compounds, e.g., Sn(II)O, gives rise to the electronic configuration of a lone pair (LP), and hence makes these compounds favorable candidates to undergo pressure-induced insulator-metal (IM) transitions at modest pressures.^{3,4} SiO is commercially available as an amorphous bulk and its high-pressure properties can be compared to those of its analogs. A pressure-induced insulator to metal transition in amorphous SiO was observed at a pressure of ~ 12 GPa by using optical and electrical probes. Short-range order on the molecular scale helps us explain the IM transition in terms of the Anderson theory of localization,⁵ where LP electrons create states in the gap.⁶ The LP wave functions are localized near individual atoms at low concentration, but as the pressure is increased atoms approach one another and the overlap of wave functions spreads their levels into bands. At some critical pressure, a certain value of the nonbonding electron concentration is achieved and these states become delocalized. Raman and ir spectroscopies reflect the response to high pressure of bond-bending and bond-stretching modes in a network of SiO molecules.

II. EXPERIMENTAL PROCEDURE

Pressure-dependent ir and Raman spectroscopy, temperature-dependent electrical resistance measurements (TDERMs), and x-ray scattering on SiO (99.99%, commercially available from Pfaltz & Bauer) were carried out using a diamond anvil cell (DAC) with 500 μm culets. The sample chunks were hand milled in an agate mortar. We used a 301

stainless steel gasket, indented to 50 μm thickness, and a sample cavity of 150 μm diameter. The ruby luminescence method⁷ was used to measure the pressure. For the ir and Raman experiments, we used polyethylene powder for hydrostatic conditions. For x-ray scattering measurements, nitrogen was used as the pressure medium. TDERMs were carried out using a sandwiched gasket.⁸ We sandwiched two back-to-back preindented 125- μm -thick steel gaskets with a 10 μm mica sheet using Araldite epoxy. A cavity was drilled through the three-layered gasket, and copper electrodes were soldered to the upper and lower layers in a two-point probe configuration. The x-ray (wavelength 0.4101 \AA) scattering was measured at the ID9 beamline of ESRF (the European Synchrotron Radiation Facility, Grenoble). The DAC was tilted $\pm 3^\circ$ in order to get better averaging of the powder diffraction. The FIT2D software⁹ was used to convert the images into 2θ diagrams. ir spectra were taken at LENS (the European Laboratory for Nonlinear Spectroscopy, Florence), using a Bruker 120HR interferometer with a 6 μm Mylar beam splitter and a bolometer. Raman backscattering spectra were collected at BGU (Ben-Gurion University, Beer-Sheva). The excitation line of 632.8 nm was focused on the sample by a 50 \times objective optical microscope, and a Jobin-Yvon 800 triple-grating spectrometer coupled to a charge-coupled device was used for the Raman data.

III. RESULTS

A. X-ray diffraction

The glassy nature of SiO at ambient and high pressure was shown by a set of x-ray scattering experiments. X-ray data were collected up to 30 GPa. The empty DAC background was subtracted from the data. As typical for noncrystalline materials, continuous scattering patterns with no diffraction peaks were obtained. Some representative diffraction patterns are presented in Fig. 1.

B. Vibrational spectroscopies

Breaking of the selection rules at $\Delta\vec{K}$ in amorphous materials¹⁰ causes similarity in the ir and Raman spectra at ambient conditions: the 469 cm^{-1} Raman phonon vs the 466 cm^{-1} ir phonon. The broadbands observed in these two

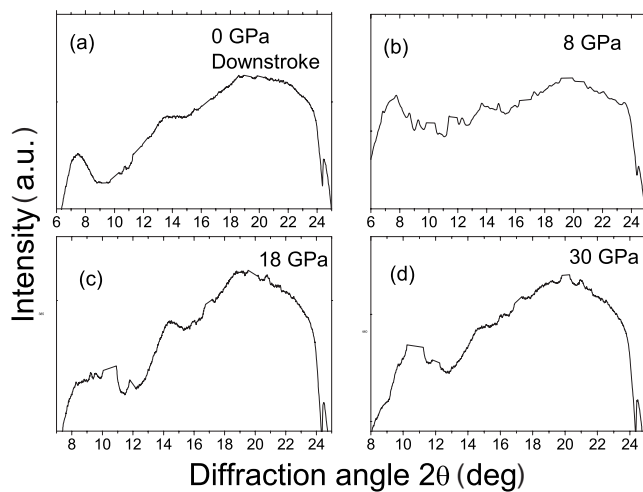


FIG. 1. x-ray scattering patterns of SiO powder at (a) 0, (b) 8, (c) 18, and (d) 30 GPa download. Broad features with no sharp peaks are shown, as expected from a noncrystalline material. The background from the DAC and the gasket has been subtracted.

probes are also attributed to the breaking of selection rules. Ir spectra were collected up to ~ 28 GPa in the spectral range of $400\text{--}700\text{ cm}^{-1}$. The effective thickness of the sample changes with pressure; therefore we use the optical density $O_d(\nu) = \ln[I_0(\nu)/I(\nu)]$, where $I_0(\nu)$ is the measured intensity transmitted by a pure polyethylene pellet and $I(\nu)$ is the intensity transmitted by the sample together with the polyethylene pellet. The measured $O_d(\nu)$ of SiO at several high pressures is shown in Fig. 2.

The Raman spectrum at ambient pressure of a sample that underwent the metallic transition shows that the metallic characteristic is preserved after pressure is released, as shown in Fig. 3. Thus the amorphous metal can be considered as a long-lived metastable phase at ambient conditions, on a time scale of months.

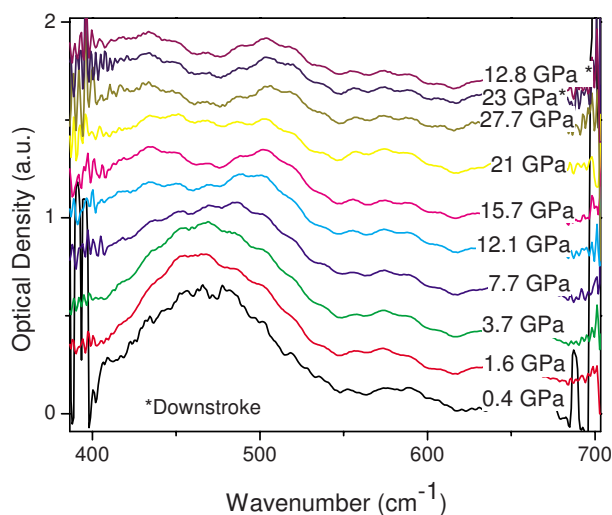


FIG. 2. (Color online) Optical density measured by ir transmission at several pressures. The phonon at $\sim 466\text{ cm}^{-1}$ is submerged as the overall absorption increases with pressure. An asterisk near the pressure signifies measurement downstrokes.

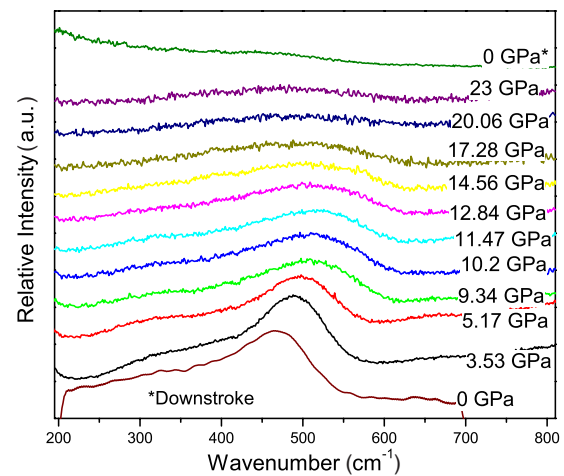


FIG. 3. (Color online) Raman scattering spectra of SiO at different pressures. A wide band centered at 469 cm^{-1} is blueshifted with the pressure, indicating phonon stiffening. The excitation line is of wavelength 632.8 nm . Downstroke spectrum at ambient conditions (denoted by an asterisk) was taken outside the DAC long after the pressure was released.

C. Electrical measurements

For TDERMs we used the sandwiched gasket described above. The DAC was mounted on a cold finger operated between 100 and 300 K for each isobar. The pressure and temperature dependencies of the resistance at room temperature are shown in Figs. 4 and 5, respectively. A dramatic drop of nine orders of magnitude in the resistance is observed around 12 GPa, indicating a discontinuous transition from semiconductor to metal.

Our electrical measurements under high pressure exhibit three different temperature dependencies of the resistance, as shown by the isobars in Fig. 5. On the metallic side of the transition ($P \geq 12$ GPa), the resistance dependence on the temperature is weak (within the range of $1\ \Omega$ vs an initial

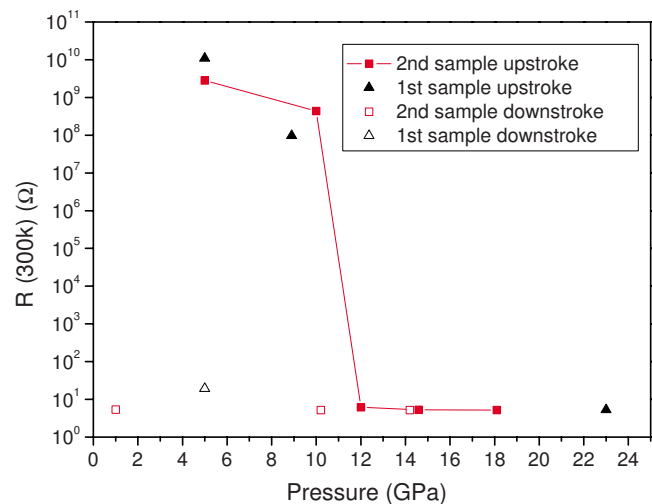


FIG. 4. (Color online) Pressure dependence of the resistance for two SiO samples. The IM transition is clearly seen at a pressure of 12 GPa.

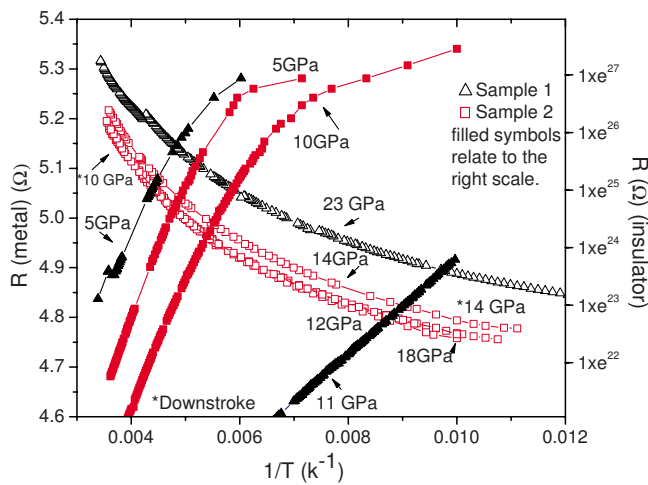


FIG. 5. (Color online) Variation of electrical resistance as a function of reciprocal temperature for two SiO samples. Left-scale curves relate to the metallic state where weak dependence on the temperature is observed. Right-scale curves describe the insulating state, where the temperature dependence of the resistance is strong. A change of slope is seen at ca. 150 K, indicating different conduction mechanisms. These measurements were taken in nonhydrostatic conditions.

value of $\sim 5 \Omega$). The conductivity decreases with increasing temperature. This type of behavior is expected in amorphous metals,¹¹ where $l \gg a$ (l is the electron mean free path and a is the interatomic distance), and therefore it can be described by the Ziman formula for liquid metals.¹² On the insulating side of the transition (right scale in Fig. 5), Ziman's theory is not applicable, since $l \sim a$ and high glass resistivity, which decreases dramatically with increasing temperature, is observed. Furthermore, on this side a change in the temperature dependency of the resistance is exhibited, implying different conduction mechanisms. This will be discussed elsewhere.

IV. DISCUSSION

In Fig. 2, the low-pressure ir peak at $\sim 466 \text{ cm}^{-1}$ is submerged at around 12 GPa by a gradually rising background attributed to higher reflectance due to free electrons. The Raman peak is diminished as well for the same reason. This can be seen in Fig. 3. One can distinguish between the pressure dependencies of the ir absorption band and of the Raman scattering band. While in the Raman spectra hardening or blueshift of the band is observed with increasing pressure, in the ir spectra the absorption band does not shift. The broad peaks in the ir and Raman spectra are a result of a weighted summation over all band modes, namely, the phonon density of states.¹⁰ Some modes in the Raman activity may be more intense at one pressure than at another. Amorphous SiO is expected to have a two-dimensional network, with no medium-range order.¹³ Densification of such a network causes tetrahedral units to move closer together, mainly by bending of bonds, since its force constants are generally smaller than the central force constants of bond stretching. Both Raman modes, which are activated by induced polarizability, and ir modes, which are activated by dipole moments,

are linear with displacement of atoms joined by a bond, and hence with bond length. Yet there is a difference in the origin of activation between the two optical probes. On the one hand, in-phase compression of neighboring bonds intensifies the activity of Raman modes—bending of one bond can induce symmetric stretch¹⁴ on its neighboring bonds, and the breathing movement of neighboring atoms activates Raman modes. On the other hand, pure stretching of bonds can compress one bond while its neighbor is extended. This antisymmetric motion is expected to result in an ir-active mode. Putting the above arguments together, it is reasonable to assign the Raman-active modes to bends, since they are hardened under pressure, whereas ir-active modes are dominated by stretches, since their matrix element is not affected by pressure. Gradual broadening of the main line observed in the optical density spectra (Fig. 2) indicates that the distribution of bond stretching modes increases with pressure. It is reasonable to assume that the electronic structure of Si, Pb, and Sn monoxide compounds is similar. Therefore, a compound of Si with a chalcogen can form a band of LPs. Calculations of the electronic structure of crystalline SnO and PbO (Refs. 15 and 16) have confirmed that in these compounds cation s LP states hybridize with O p states. In this case, LP electrons play the main role in creating bonding and antibonding combinations, which stabilize the litharge structure of SnO and PbO upon interaction with cation p states. However, in the noncrystalline case of SiO, to enable the IM transition, LP electrons must not take part in chemical bonding, and therefore the “classical” hybridization theory for LPs as being nonbonded¹⁷ is suitable. The electronic configuration of a Si atom is $3s^23p^2$, and $2s^22p^4$ for an O atom. The electronegative O atom will capture two electrons from the outer shell of the Si atom, changing the electronic configuration into $3s^23p^0$ and $2s^22p^6$ for Si and O atoms, respectively. The two $3s$ electrons of Si become a LP upon hybridization of s and p states of the cation. Considering SiO as an admixture of oxygen in amorphous silicon, then the origin of LP electrons is the oxygen; upon reaction with the hosting solid amorphous silicon, it creates bonding, nonbonding, and antibonding bands, as in LP semiconductors.⁶ We believe that in these cases the LP states fall in the gap between valence and conduction bands. Diminution of the distance between nearest neighbors by high pressure will broaden the bonding and antibonding bands until a complete closure of the gap is achieved. In addition, the concentration of LP electrons will continuously increase with pressure. An Anderson transition is expected when a critical value of LP electron concentration is exceeded, and delocalization of these states takes place. The pressure-induced discontinuity in conduction, which is characteristic of an Anderson transition, was observed by electrical measurements as described above.

A dramatic drop of the resistance (Fig. 4) and a sign change in the temperature dependence of the resistance (Fig. 5), both happening at ~ 12 GPa, fit an Anderson transition. Moreover, on each one of the isobars in Fig. 5, going from the high-temperature to the low-temperature region, a cross-over from steep exponential to a slower dependence on the temperature is observed. This behavior can be attributed to the changes in the temperature dependence of the conductivity, as described above.

V. SUMMARY

At ~ 12 GPa SiO undergoes a transition from an amorphous insulator to an amorphous metal. As seen in the ambient Raman spectrum, a long-lived metastable phase is formed, which preserves its metallic characteristics long after the transition pressure is released. This is in correlation with our findings in the electrical measurements. X-ray scattering patterns taken up to ~ 30 GPa confirm that this compound is noncrystalline throughout this pressure range. *ir* and Raman spectroscopies show broadbands, characteristic of amorphous insulators, up to the transition pressure, and flattened spectra, characteristic of metals, above this pressure. TDERMs show a sharp transition from insulator to metal. The metallic behavior qualitatively fits the Ziman formula for liquid metals. The insulator has two different temperature regimes, in agreement with the Mott-Anderson theory. Details will be presented elsewhere. The two

probes—vibrational excitation spectroscopies and electrical measurements—yield two viewpoints on the pressure-induced processes in amorphous SiO. On the one hand, the *ir* and Raman spectra indicate that the closure of the band gap is continuous with increasing pressure due to short-range order. On the other hand, a sharp change in the electronic properties of SiO, characteristic of an Anderson transition, is observed from the pressure and temperature dependencies of its resistance. The theory of LPs in semiconductors is applied to describe the observed pressure-induced IM transition. The origin of the LP states is still a puzzle for us. This reflects the debate in the literature on SiO: as a compound it is reasonable to ascribe formation of LP electrons to the electronic configuration of group-IV monoxides, whereas, considering it as a mixture, LP formation should be ascribed to the bonding of the amorphous group-IV element with chalcogen atoms. Soft x-ray spectroscopy may resolve this issue of the IM transition and structural properties of SiO.

-
- ¹S. M. Schnurre, J. Grobner, and R. Schmid-Fetzer, *J. Non-Cryst. Solids* **336**, 1 (2006).
- ²T. Chattopadhyay, A. Werner, and H. G. von Schnering, in *High Pressure in Science and Technology*, edited by C. Homan, R. K. MacCrone, and E. Whalley, MRS Symposia Proceedings No. 22 (Materials Research Society, Pittsburgh, 1984).
- ³N. E. Christensen, A. Svane, and E. L. Peltzer y Blancá, *Phys. Rev. B* **72**, 014109 (2005).
- ⁴E. Sterer, M.Sc. thesis, Tel-Aviv University, 1989.
- ⁵P. W. Anderson, *Phys. Rev.* **109**, 1492 (1958).
- ⁶M. Kastner, *Phys. Rev. Lett.* **28**, 355 (1972).
- ⁷G. J. Piermarini, S. Block, J. D. Barnett, and R. A. Forman, *J. Appl. Phys.* **46**, 2774 (1975).
- ⁸D. Leong, H. Feyrit, A. D. Prins, V. A. Wilkinson, K. P. Home-wood, and D. J. Dunstan, *Rev. Sci. Instrum.* **63**, 5760 (1992).
- ⁹A. P. Hammersley, S. O. Svelsson, M. Hanfland, A. N. Fitch, and D. Haussermann, *High Press. Res.* **14**, 235 (1996).
- ¹⁰R. Shuker and R. W. Gammon, *Phys. Rev. Lett.* **25**, 222 (1970).
- ¹¹N. F. Mott, *Metal-Insulator Transitions* (Taylor and Francis, London, 1990).
- ¹²J. Ziman, *Philos. Mag.* **6**, 1013 (1961).
- ¹³A. Hohl, T. Wieder, P. A. van Aken, T. E. Weirich, G. Denninger, M. Vidal, S. Oswald, C. Deneke, J. Mayer, and H. Fuess, *J. Non-Cryst. Solids* **320**, 255 (2003).
- ¹⁴F. L. Galeener, *Phys. Rev. B* **19**, 4292 (1979).
- ¹⁵G. W. Watson and S. C. Parker, *J. Phys. Chem. B* **103**, 1258 (1999).
- ¹⁶A. Walsh and G. W. Watson, *Phys. Rev. B* **70**, 235114 (2004).
- ¹⁷I. Lefebvre, M. Lannoo, G. Allan, A. Ibanez, J. Fourcade, J. C. Jumas, and E. Beaurepaire, *Phys. Rev. Lett.* **59**, 2471 (1987).